CFD analysis of spar vortex-induced motions in uniform and sheared flows

Weiwen Zhao, Decheng Wan

State Key Laboratory of Ocean Engineering, School of Naval Architecture, Ocean and Civil Engineering, Shanghai Jiao Tong University, Collaborative Innovation Center for Advanced Ship and Deep-Sea Exploration
Shanghai, China
* Corresponding author: dcwan@sjtu.edu.cn

ABSTRACT: Spar offshore platform, characterized by its deep draft with vertical columnar hull shape, is subject to Vortex-Induced Motions (VIM). The hurricane and loop current, whose velocity profile are highly non-uniform along the vertical direction, are common current events in the Gulf of Mexico. The present study numerically investigates the VIM response of a Spar platform in uniform and sheared currents based on a Computational Fluid Dynamics (CFD) approach. The incompressible finite volume solver naoe-FOAM-SJTU is used for all the computations and the Detached-Eddy Simulations (DES) is selected for turbulence closure. Moreover, the effects of different reduced velocities on VIM response are also discussed.

KEY WORDS: Spar; vortex-induced motions (VIM); detached-eddy simulation (DES); sheared current; naoe-FOAM-SJTU solver

INTRODUCTION

Vortex-induced motions (VIM) is a unique dynamic response to currents for deep-draft floating bluff platforms such as Spars, semi-submersibles and TLPs. Among them is the spar platform, which is typically a vertical immersed vertical cylinder about 40m in diameter with a draft of 200m, moored to the seabed with a catenary mooring system. VIM is in fact the resonant motion of the offshore platform as a result of the periodic transverse pressure by vortex shedding from both sides of the hull. VIM will particularly have large response when the vortex shedding frequency is approaching natural frequency of the platform mooring system. The vortex will shed at a frequency equal to one natural frequency in a range of different velocities, which is referred as “lock-in”. Due to the large motion response and long period (comparing to Vortex-Induced Vibration, or VIV), VIM will more considerably result in extreme tension and fatigue damage to the risers and mooring lines. For this reason, it is important to predict the VIM characteristics accurately and provide key information for designing of the risers and mooring system.

In tradition, model tests are performed to investigate the VIM characteristics before design phase. These tests are conducted in a towing tank, ocean basin or flume. Due to the size limitation of physical experiment, typical model scale ratios are 1:40 or higher. Hence the Reynolds numbers for typical Spar VIM model tests are limited in the order of 10^4 or 10^5. Full scale Spar Reynolds numbers are up to 10^7. Froude scaling is used for model tests. Recent advances of computer science and numerical methods brings hope to simulate VIM by means of Computational Fluid Dynamics (CFD). The unparalleled advantages of CFD frees the constraint of physical experiment. Requirements such as long sampling time, high current speed, and stratified flows, which is difficult to achieve in model test, is easy to implement in numerical simulations. CFD is becoming one of the most important research method along with model test for studying VIM characteristics.

This paper performs numerical test for Spar VIM in different current profiles, i.e., uniform and sheared current. VIM characteristics of two current profiles are given and discussed. Some details of flow visualization are also analyzed. All the simulations are performed by our in-house solver naoe-FOAM-SJTU[11-14], which is an incompressible CFD solver based on the open source CFD toolbox OpenFOAM.

NUMERICAL METHOD

Turbulence Model

Detached-Eddy Simulation (DES) is a hybrid RANS/LES method which combines the best parts of RANS and LES, i.e., employs RANS model in near-wall regions to reduce grid cost and LES sub-grid scale model in other regions to better model the unsteady turbulent flow characteristics. The DES model used in this paper is based on Menter's two-equation SST turbulence model [1]. The turbulent flow is governed by the incompressible continuity equation and momentum equations:

$$\frac{\partial U_i}{\partial x_i}=0 \tag{1}$$

$$\frac{\partial U_i}{\partial t}+\frac{\partial}{\partial x_j}\left(U_iU_j\right)=-\frac{\partial p}{\partial x_i}+\frac{\partial}{\partial x_j}\left(\left(\nu+\nu_t\right)\frac{\partial U_i}{\partial x_j}\right) \tag{2}$$

Where, U_i is the filtered or time-averaged velocity field, ν is the kinematic viscosity, ν_t is the eddy viscosity. Note that in OpenFOAM, the pressure for incompressible flow is normalized by density (i.e., pressure divide by density). To determine ν_t, two more equations are introduced.

$$\frac{\partial k}{\partial t}+\frac{\partial (u_jk)}{\partial x_j}=\tilde{G}-\beta^*\omega k\cdot F_{DES}+\frac{\partial}{\partial x_j}\left[\left(\nu+\alpha_k\nu_t\right)\frac{\partial k}{\partial x_j}\right] \tag{3}$$

$$\frac{\partial \omega}{\partial t}+\frac{\partial (u_j\omega)}{\partial x_j}=\gamma S^2-\beta\omega^2+\frac{\partial}{\partial x_j}\left[\left(\nu+\alpha_\omega\nu_t\right)\frac{\partial \omega}{\partial x_j}\right]+\left(1-F_1\right)CD_{k\omega} \tag{4}$$

The DES form modifies k-equation by multiplying dissipation term by a coefficient F_{DES}. The coefficient F_{DES} is defined as

$$F_{DES}=\max\left(\frac{L_t}{C_{DES}\Delta}\left(1-F_S\right),1\right) \tag{5}$$

Where, $L_t=\sqrt{k}/\left(\beta^*\omega\right)$ is the computed turbulent length scale, $\Delta=\sqrt[3]{\Delta x\Delta y\Delta z}$ is grid size, C_{DES}=0.61 is the calibrated DES constant, F_S is blending function in SST turbulence model. Details of the SST-DES model can be referred to [2,3].

Six-degrees-of-freedom (6DoF) Model

The motion equations are solved by a 6DoF motion solver [4,5], which will be briefly introduced below. To solve the motion of a rigid body, two right-handed coordinate systems are introduced. One is the earth-fixed inertial coordinate system, and the other is rigid body fixed non-inertial coordinate system. These two coordinate systems are coupled with each other by the Euler angles of the rigid body [5,6]. The forces and moments are computed in the inertial system and transform to non-inertial system. After the rigid body motion equations are solved in non-inertial system, the acceleration and velocity, as well as displacement are obtained. In addition, any DoFs can be constrained in the solver. It is to be noticed that typical model tests are at low Froude numbers, thus the free surface is neglected and the Spar is constraint in the horizontal plane, i.e., only sway and surge are allowed during computation.

Dynamic Mesh

In order to handle the moving boundary of the Spar hull, the dynamic mesh is employed. We utilize a moving-mesh approach[7] by solving the Laplacian equation of the velocities of the moving points. In this approach, the topology of grid is maintained, mesh is allowed to deform and stretch according to the moving boundary of hull.

Mooring System

The full scale Spar platform in production is always moored to the seabed by a bunch of catenary mooring lines. In model test, however, it is not practical to model the geometrical scaled mooring system due to the limitation of water depth in ocean basin. Moreover, the current generation in ocean basin is high costly and cannot achieve high current speed. A common alternative is the towing experiment, in which, the Spar model is connected to the carriage by cables and springs. These cables and springs are often uniformly distributed around the model to achieve isotropic mooring stiffness. In CFD simulations we employ taut mooring lines to model the actual cables and springs. Each line has an anchor point which is fixed during computation, and a mooring point which is moving with spar on hull. The stiffness and pretension of the taut mooring lines are carefully adjusted in order to ensure the free-decay oscillation period is consistent with model test.

CASE CONDITION

Geometry and Mesh

The model in the current study is the hard tank section of a typical Truss Spar with a scale ratio of 1:22.3. Fig. 1 Shows the geometry of Spar model. The diameter *D* of the model Spar hull 1.75m and the draft *H* is 2.95m. Spar is equipped with helical strakes around the Spar hull. The strakes are a typical 3-start design uniformly distributed in three directions with 120 degree included angle between any two directions. The strakes height and pitch are 13% and 4 of the hull diameter. Summary of the Spar parameters is listed in Table 1.

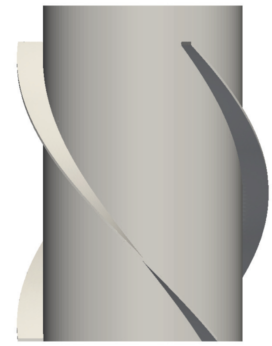

Fig. 1 Geometry of spar model

Table 1 Main particulars of Spar model [8]

Parameter	Notation	Value
Scale ratio	λ	1:22.3
Diameter	D	1.75 m
Draft	H	2.95 m
Helical strakes		3 start, 13% D height 4 D pitch
Mass	M	7088 kg
Global spring stiffness	K	2111 N/m
Linear damping	B	2.8 kg/s
Natural period of sway and surge	T_n	16.4 s

The computational domain extends to $10D < x < 17D$, $-5D < y < 5D$ and $-3H < z < 0$, as shown in Fig. 2. The grid is generated by an automatic polyhedral mesh generation tool utility provided by OpenFOAM. The mesh is generated based on a simple and orthogonal background mesh, splitting one hexahedral cell into 8 split-hexahedra cells and finally snap to the STL geometry. The total mesh is approximately 900 000 polyhedral cells. See Fig. 3 for mesh details. The boundary conditions are set as follows: free stream velocity for inlet, pressure equals zero for outlet, symmetry for sides and top, slip for bottom. Wall functions are used to reduce mesh cost. The average y+ around hull surface is about 60 which fit the requirement of SST RANS model.

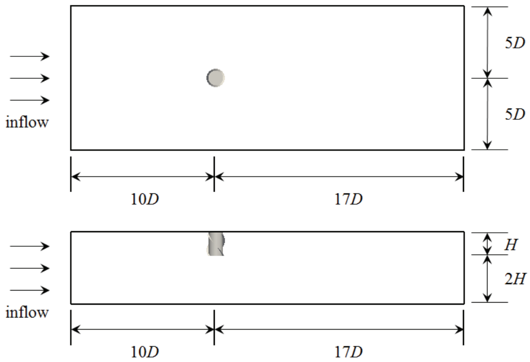

Fig. 2 Computational domain

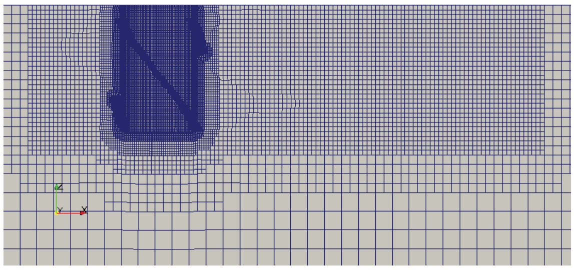

Fig. 3 Computational mesh in the vicinity of Spar model

The mooring system is modeled by 4 linear spring uniformly distributed around Spar hull with pretension. A small utility is written for static offset test in order to obtain the global stiffness. The utility reads mooring lines parameters, move rigid body along a specified direction and calculate the restore force provided by the mooring system. The global stiffness of the system is adjusted to be equal to the one obtained in static offset tests in model experiments by setting linear stiffness and pretension for each mooring line. Free decay test is performed after setting the correct stiffness and pretension for each mooring line in order to verify the natural oscillation period of the mooring system.

Current Profile

All Spar platforms has its unique design, as well as current profile in its installation place. The Gulf of Mexico, in which most Spars in production have been installed, has its specific current characteristics. Two main vertical current profile are Hurricane and Loop current. Fig. 4 shows the velocity profile of these two events. The Hurricane current, which is driven by a hurricane event, often involves high current speed and have a relatively shallow profile depth, i.e. about 65m under waterline, which is smaller than typical Spar draft. Modeling the Spar in uniform current does not represent the characteristics of a Hurricane current profile. For this reason, numerical test in sheared current should be performed in order to investigate the VIM response.

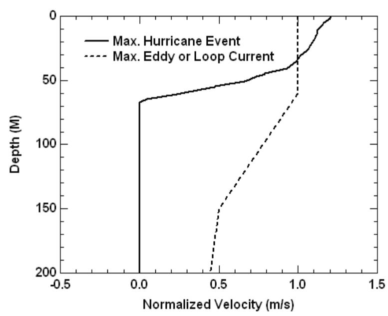

Fig. 4 Typical current profile in the Gulf of Mexico [9]

Two series of tests were performed. VIM tests for uniform current profile were carried out first. The reduced velocity, $U_r = UT_n/D$, is varied from 6 to 8, which typically fall into the "lock-in" range. For sheared current, a linear velocity which varies from maximum at z-0 to zero at z=-2 along vertical directions is applied. Three different maximum velocities in sheared current correspond to reduced velocity 6 to 8, respectively, is used.

All the calculations are carried out using the CFD solver naoe-FOAM-SJTU[11-14]. The simulations were performed on a Linux cluster with 40 Intel(R) Xeon(R) CPU E5-2680 v2 CPU cores, or 2 nodes which contains 20 CPU cores per node. The time step is 0.04s and is discretized with a 2nd order implicit scheme. 300 seconds or 18 vortex shedding cycles were calculated for each case.

RESULTS

The result for sway decay test is shown in Fig. 5. The natural period is 16.12s, which shows good agreement (1.7 E%D) with experiment.

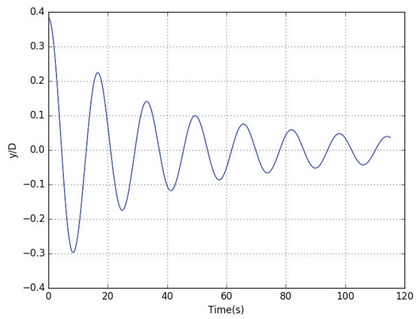

Fig. 5 Time history of sway in free decay test

Fig. 6 illustrates the velocity magnitude contour of flow for uniform and sheared current in the *xz* plane through the centroid of the Spar. The left figure shows a high gradient of velocity magnitude at the bottom of the Spar hull for uniform current, indicating the existence of high pressure. A recirculate region is observed at the free-end plane of Spar in the right figure. Vortex sheds at both sides of Spar hull as well as at free-end plane.

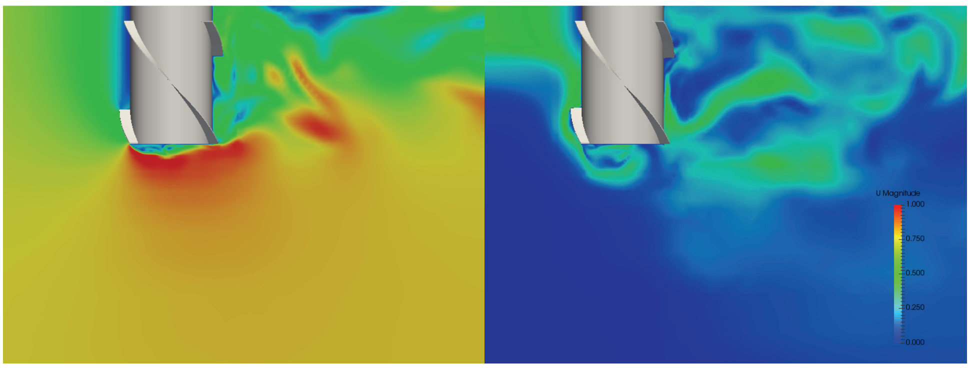

Fig. 6 Instantaneous velocity magnitude contour: uniform (left) and sheared (right) current

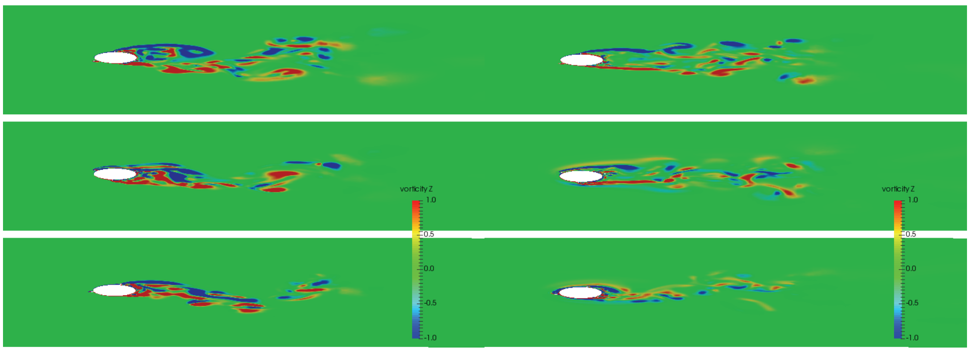

Fig. 7 Instantaneous vorticity contour: uniform (left) and sheared (right) current

Fig. 7. shows the difference of wake pattern along vertical direction between uniform and sheared currents. The contour is presented by three slices (*z*=-0.5/-1.5/-2.5m). The vortical structure is much stronger for uniform compared with sheared current. Note that in the case of sheared current, vortex even sheds below *z*=-2 where the flow velocity is zero.

The nominal maximum A*, defined as square root of 2 times the RMS (root mean square) of non-dimensional motion time series, was proposed to evaluate VIM [10]. Fig. 8 shows the nominal maximum at different velocities. The VIM response is much higher for uniform compared with sheared current. This is due to the large-scale detached eddies from both sides of the hull, which can be observed from Fig. 7. To validate the turbulence model, an extra run by using the Spalart-Allmaras Delayed Detached Simulation (SA-DDES) is performed. The result of SA-DDES shows in good agreement with the present SST-DES turbulence approach.

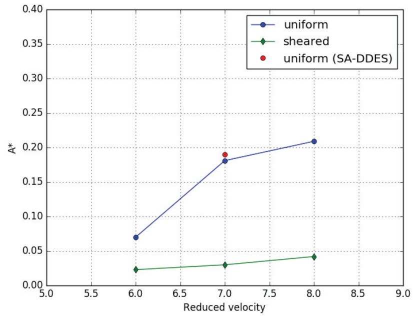

Fig. 8 Nominal maximum at different reduced velocities

CONCLUSIONS

In this paper, VIM simulations of a Spar hard tank at model scale in uniform and sheared currents are performed. All computations are carried out by our in-house CFD solver naoe-FOAM-SJTU. To model flow past bluff body, turbulence model is a key factors. We implemented the SST-DES model into naoe-FOAM-SJTU and use it along with wall functions to handle massively separated flow and reduce computational cost. We compared SST-DES with SA-DDES and the result shows slight difference. Our CFD results show sophisticated flow around the complex geometry. The flow pattern of VIM in sheared current behaves very different from uniform current. Smaller VIM response is observed in sheared current, which shows that predicting VIM in uniform current is slightly conservative.

Despite the effort of current study, a great deal of work remains, in which the most important one is the effect of turbulence model at high Reynolds numbers. High Reynolds number flows with complex geometry remains a great challenge for CFD community. More basic benchmark with simpler geometry should be carried out in the future work to study the role of turbulence model in industrial flows.

ACKNOWLEDGEMENTS

This work is supported by the National Natural Science Foundation of China (51379125, 51490675, 11432009, 51579145, 11272120), Chang Jiang Scholars Program (T2014099), Program for Professor of Special Appointment (Eastern Scholar) at Shanghai Institutions of Higher Learning (2013022), Innovative Special Project of Numerical Tank of Ministry of Industry and Information Technology of China (2016-23/09), to which the authors are most grateful.

REFERENCES

[1] MENTER F R. Two-equation eddy-viscosity turbulence models for engineering applications[J]. AIAA Journal. 1994, 32(8): 1598–1605.
[2] MENTER F R, KUNTZ M, LANGTRY R. Ten years of industrial experience with the SST turbulence model[J]. Turbulence, Heat and Mass Transfer. 2003, 4(1): 625–632.
[3] ZHAO W, WAN DC. Numerical study of 3D flow past a circular cylinder at subcritical Reynolds number using SST-DES and

SST-URANS[J]. Chinese Journal of Hydrodynamics. 2016, 31(1): 1–8.

[4] SHEN Z, WAN DC. Numerical simulation of sphere water entry problem based on VOF and dynamic mesh methods[C]. Proceedings of the 21st International Offshore and Polar Engineering Conference (ISOPE), Maui, Hawaii, USA, June 19-24, 2011: 695-702.

[5] SHEN Z, WAN DC. RANS computations of added resistance and motions of a ship in head waves[J]. International Journal of Offshore and Polar Engineering. 2013, 23(4): 263–271.

[6] CARRICA P M, WILSON R V, NOACK R W, et al. Ship motions using single-phase level set with dynamic overset grids[J]. Computers & Fluids. 2007, 36(9): 1415–1433.

[7] JASAK H. Dynamic mesh handling in OpenFOAM[C]. 47th AIAA Aerospace Sciences Meeting including the New Horizons Forum and Aerospace Exposition. Orlando, Florida, USA, 2009.

[8] FINNIGAN T, RODDIER D. Spar VIM model tests at supercritical reynolds numbers[C]. Proceedings of the 26th International Conference on Offshore Mechanics and Arctic Engineering-OMAE. San Diego, California, USA, 2007, 3: 731–740.

[9] OAKLEY O, CONSTANTINIDES Y, NAVARRO C, et al. Modeling Vortex Induced Motions of spars in uniform and stratified flows[C]. Proceedings of the 24th International Conference on Offshore Mechanics and Arctic Engineering-OMAE. Halkidiki, Greece, 2005: 5–67238.

[10] OAKLEY JR. O H, CONSTANTINIDES Y. CFD truss spar hull benchmarking study[C]. Proceedings of the 26th International Conference on Offshore Mechanics and Arctic Engineering - OMAE. San Diego, California, USA, 2007, 3: 703–713.

[11] SHEN Z, WAN DC and CARRICA P. Dynamic overset grids in OpenFOAM with application to KCS self-propulsion and maneuvering[J]. Ocean Engineering, 2015, 108: 287-306.

[12] SHEN Z, WAN DC. The manual of CFD solver for ship and ocean engineering flows: naoe-FOAM-SJTU[R]. 2014: Shanghai Jiao Tong University.

[13] SHEN Z, WAN DC. An irregular wave generating approach based on naoe-FOAM-SJTU solver[J]. China Ocean Engineering, 2016, 30(2): 177–192.

[14] CAO H, WAN DC. Development of Multidirectional Nonlinear Numerical Wave Tank by naoe-FOAM-SJTU Solver[J]. International Journal of Ocean System Engineering, 2014, 4(1): 52–59.